JOURNAL OF MATERIALS SCIENCE 24 (1989) 3002–3010

Structure of oxide gels and glasses by infrared and Raman scattering

Part 1 *Alumina*

Ph. COLOMBAN
Laboratoire de Physique de la Matière Condensée, Chimie du Solide UA 1254 – CNRS, Ecole Polytechnique, 91128 Palaiseau, and Laboratoire de Spectrochimie IR et Raman, CNRS, 2 rue H. Dunant, 94320 Thiais, France

Optically clear monolithic gels and fine gel powders have been synthesized using various alkoxide hydrolysis reactions. The gels have been characterized using various methods to determine their structures. (X-ray diffraction, DTA, TGA, DSC, IR and Raman spectroscopies). The spectra and the nature of gels depend on the solvent and the hydrolysis conditions (rate, pH, etc.). The use of acetone as solvent allows reduction of the hydrolysis time, from weeks to hours. If the hydrolysis of aluminium sec-butoxide is too rapid, at high pH, crystalline bayerite $Al(OH)_3$ is formed. Regular hydrolysis leads to amorphous optically clear gel with sometimes boehmite (or diaspore) traces. Formation of the (porous) glass (300 to 600° C) and also of the γ-alumina does not modify the Raman spectra strongly whereas large modifications are observed on IR spectra with the evolution of protonic species. The structure of alumina gel and glass is of the spinel type. The α-alumina phase grows above 1200 to 1250° C (above 1050° C if boehmite traces are present).

1. Introduction

Preparation of monolithic gels and glasses as well as fine powders and ceramics through sol–gel methods and alkoxide hydrolysis have attracted considerable attention in recent years [1–4]. Gel routes offer specific advantages (e.g. low sintering temperature and fine microstructure, high homogeneity, etc.) to prepare fine powders as well as monoliths leading to well-densified, glass-ceramics or ceramics [5–9]. Thus, it is possible to choose the sintering temperature and the degree of crystallinity of various compositions [9, 10]. A great number of publications concern SiO_2 or SiO_2-rich compositions [1–4, 7, 8] but only a few papers are devoted to alumina [11–13].

The Raman spectroscopy has been recently used in some works in order to check the hydrolysis–polycondensation of SiO_2 [14–17]. Attempts to understand the local structure of gels concern SiO_2 aerogel [18]. In this paper we discuss the local structure of gels, "glasses" and poor crystallized aluminas (usually called "transition aluminas") using X-ray diffraction, differential thermal analysis (DTA), thermogravimetric analysis (TGA), differential scanning calorimetry (DSC), infrared (IR) and Raman spectroscopies. In subsequent papers mullite, GeO_2 and zirconia will be considered in relation to synthesis, non-stoichiometry and doping.

2. Experimental procedure

2.1. Synthesis

Two routes of synthesis have been used: the slow hydrolysis route leading to optically clear monoliths and the rapid hydrolysis route leading to fine powder. Pressing the powder allows preparation of dense transluscent pieces [6, 9].

2.1.1. Slow route

A propanol or (cyclo)hexane or acetone solution of aluminium sec-butoxide (Alfa-Ventron, Karlsruhe) was slowly hydrolysed with air moisture (relative humidity ~ 60%) (Table I). The solutions were kept in a Petri-box (diameter ~ 100 mm) or in a covered bottle (diameter ~ 30 mm, height ~ 100 mm). The respective ratio between alkoxides and solvent was between 1/1 and 1/2 (Table I). A typical batch corresponded to 100 cm^3. Atmospheric moisture reached the solution surface through very small pin-holes in the cover or through the interstices between the bottom and the cover of the Petri box. After day(s) to weeks (Table I) monolithic optically clear gels (apparently "dry" and hard) were obtained and were dried between 30 and 60° C for a week. Drying crushes the monoliths to a few pieces of about 0.1 to 1 cm^3. The pH of the solvent was modified by adding a few drops of NH_4OH, CH_3COOH, HCl or H_3PO_4.

Alumina gel was also prepared directly from the pure aluminium sec-butoxide through a very small air invasion at the bottle stopper. Months were needed to obtain optically clear monoliths (0.5 to 1 cm^3).

In comparison, monolith gel was also prepared according to the Dwivedi and Godwa method [19]. Fig. 1 shows monolithic gels obtained by both hexane and Godwa methods.

2.1.2. Rapid route

The alkoxide mixture was diluted in propanol. A large excess of water (typical alcohol/alkoxide/water volume ratio 2/1/2) was used to achieve complete hydrolysis under a rigorous mixing. The pH of the water was modified by NH_4OH or acid addition (Table I). Prior

0022–2461/89 $03.00 + .12

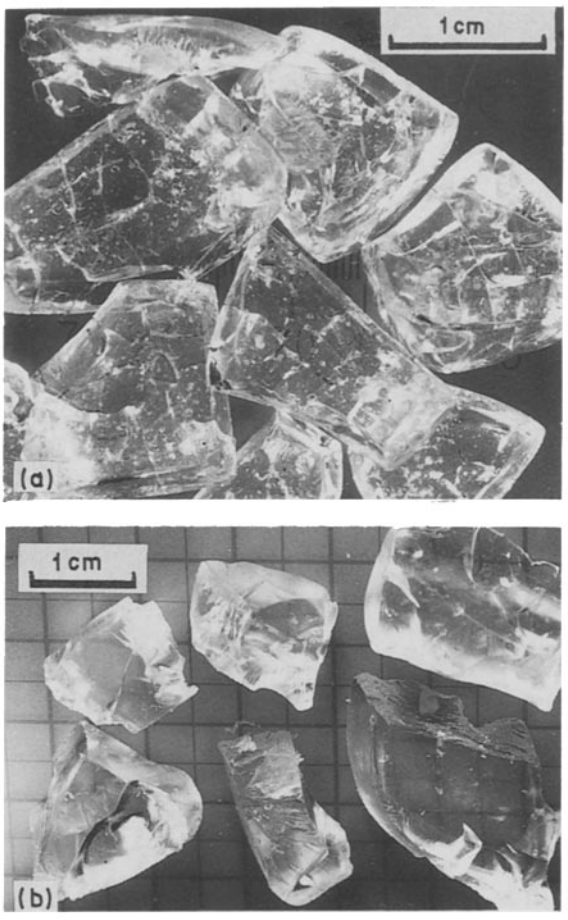

Figure 1 Monolithic gels synthesized by slow hydrolysis of aluminium sec-butoxide in (a) hexane or (b) with the Dwivedi and Godwa method [19].

to hydrolysis, the mixture was heated for 1 h at 80° C. A typical batch used 50 cm^3 alkoxide. Gel powder was obtained after room-temperature removal of water and alcohol. Manual blending was carried out during drying in order to prevent the formation of hard agglomerates. The powder was then dried at 50° C for a week and could then be compacted as previously described [9].

Note that before Raman spectra recording, it was necessary to dry the samples for a few weeks at room temperature to minimize fluorescence. Fluorescence can also be strongly decreased by exposing the sample for 1 h to a laser focus.

2.2. Characterization

The density of gels and of the thermally treated samples was measured using the usual mass and volume determination in water or in alcohol. Apparent density was also measured on pellets (diameter $\simeq$ 10 mm) prepared by powder compaction ($\simeq$ 200 kN). In the case of monolithic gels, grinding was performed in a mortar before compaction.

Thermogravimetry (TGA) was performed between 30 and 700° C (heating rate 60° C h^{-1}) with a Dupont de Nemours Instrument. Differential thermal analysis (DTA) (30 to 1500° C range) was also performed with a Dupont Instrument. Differential scanning calorimetry (DSC) traces were recorded between 0 and 400° C under a nitrogen flux using a DSC4 Perkin–Elmer apparatus. Weight loss was measured after each run. X-ray powder patterns are recorded with the λCu$K\alpha$ radiation. Infrared spectra were recorded on a 783 Perkin–Elmer spectrophotometer using paraffin oil and Fluorolube mulls between CsI, CaF_2 or KRS5 windows. Raman spectra were recorded with an Instrument S.A. Mole Microprobe associated with a 1.5 W argon ion laser (Spectra Physics). The 514.5 nm excitation was preferentially used to minimize fluorescence. An optical prism-based accessory removed the other parasitic components. Note that the ISA Mole allowed illumination and collection of the diffusion light through a microscope. Thus, the area examined was approximately a few square micrometres and the large angle of collection allowed examination of very poor scatterers in many places. The light power at the

TABLE I Synthesis of $Al_2O_3 \cdot nH_2O$ materials from aluminium sec-butoxide hydrolysis

Solvent ratio[△] (by volume)	Method and hydrolysis medium	Gelation time*	Drying time	Weight loss (%)	Density[†]	ΔH (cal g^{-1})		Remarks
						1st peak	2nd peak	
Isopropanol 2/1/2	water + NH_4OH (pH 9)	inst.	5 d 30° C	35	2.2	90	60	White, bayerite + boehmite
	water + HCl (pH 2)	inst.	3 d 30° C	60	1.9	90	–	White, boehmite
	atmospheric moisture	> 6 mon	30° C 3 d	35	1.6	60	–	Optically clear, boehmite traces
			70° C	30		80	1	
Hexane 1/1	atmospheric moisture	8 d	30° C	50	1.9	100	2.5	Optically clear, boehmite
	as above	1 d	30° C	60	1.5	–	–	traces
	+ NH_4OH	8 d	30° C	25	1.4	20	4	
	+ CH_3COOH	8 d	30° C	45	1.2	70	–	White, bayerite + boehmite
	+ HCl	8 d	30° C	45	1.6	140	–	
Cyclohexane 1/1	atmospheric moisture	8 d	30° C 3 d	40	1.5	90	1.5	Optically clear, boehmite
Acetone 2/1	atmospheric moisture	8 d	30° C	70	1.3	32	4	Optically clear, yellow
		1 d	2 d	80	1.2	90	2.5	As above
Dwivedi and Godwa [19]		4 mon	2 mon 50° C	26		60	–	Boehmite and diaspore traces

[△] Solvents ratio: solvent/alkoxide/(water).
*inst., instantaneous; d, days; mon, months.
[†] Apparent density of compacted pellets.

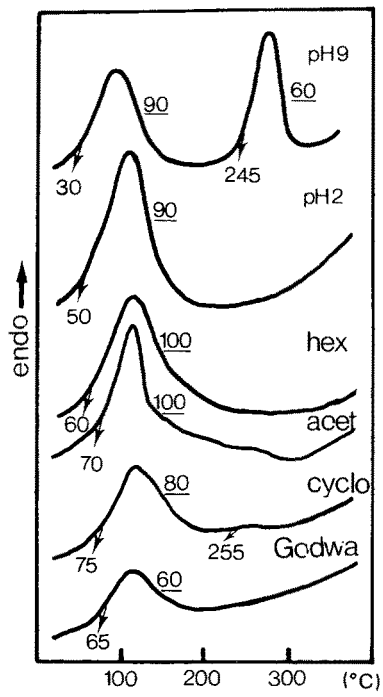

Figure 2 DSC traces of some alumina monoliths and powders: pH 9 and pH 2 powder, monoliths prepared in hexane, cyclohexane and acetone or with the Dwivedi and Godwa method (heating rate 10° C min^{-1} enthalpy (ΔH) in cal g^{-1}).

sample surface ranged between 1 and 50 mW. With our apparatus the accuracy of frequency was about $\pm 5\,cm^{-1}$.

3. Results and discussion

3.1. Evidence of various types of alumina "gels"

The aspect and shape of gels appear very different. Gels prepared by slow hydrolysis directly from butoxide or in hexane are hard and optically clear. On the other hand, Godwa [19] or Yoldas [20] gels look soft and wet. They can only be transluscent after a 100° C drying. Monoliths prepared in acetone are optically clear but yellow in colour (Table I).

Figs 2 and 3 compare DSC and TGA traces between 30 and 400° C. Three types of DSC traces can be recognized:

(i) one broad peak trace (onset temperature 50 to 70° C) corresponding to hard optically clear monoliths,

(ii) two-peak traces (onset temperature 30 and 245° C) corresponding to pH 9 gel powder.

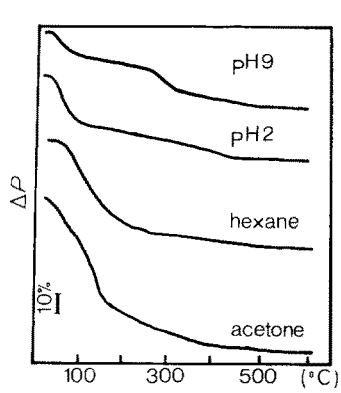

Figure 3 TGA traces of pH 9, pH 2 powders and of monoliths synthesized in hexane or in acetone.

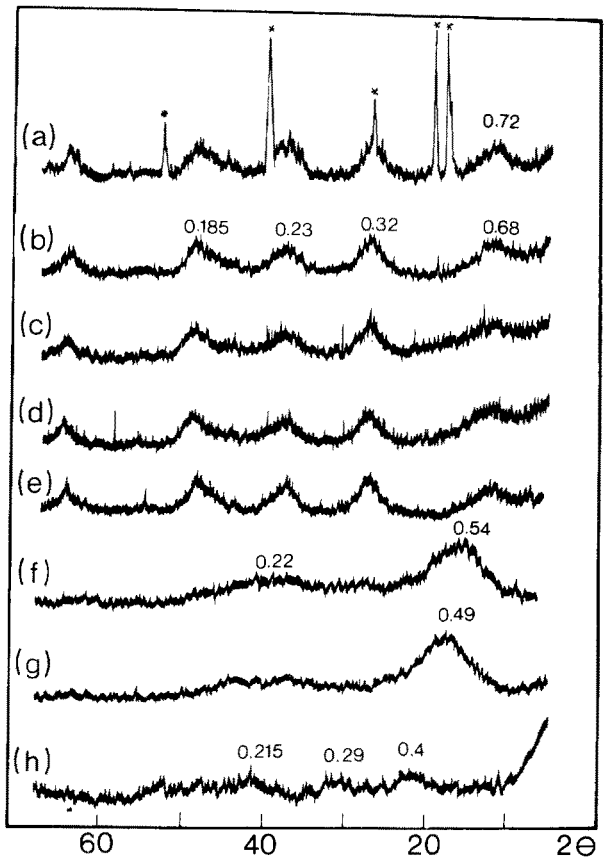

Figure 4 X-ray powder patterns (λCu$K\alpha$) of "alumina gels" in the form of: (a, b) powder from rapid hydrolysis in propanol with (a) pH 9 or (b) pH 2 water, (*) $Al(OH)_3$ phase; powdered optically clear monoliths prepared by slow hydrolysis in (c) hexane, (g) acetone or (h) propanol, or (f) by rapid hydrolysis in acetone; comparison is given with monoliths prepared by very slow hydrolysis of pure aluminium sec-butoxide (d), or from the Godwa method (e). (Interreticular distance d in nm.)

(iii) traces with very small peaks at about 220 to 250° C corresponding to an intermediate case.

The corresponding weight losses range between 25 and 35% (two peak traces) and 50 to 60% (one-peak trace). Highest weight losses (80%) are measured with yellow monoliths synthesized using acetone as solvent (Table I). Comparison of infrared spectra in the 4000 to 1000 cm^{-1} region shows that the matter lost below 400° C consists in protonic species (organic traces are only observed for gels prepared in acetone). Thus the following formulae can be proposed for the different "gels":

(i) pH 9 gel powder, monoliths made by direct Al–O–Bu hydrolysis or by slow hydrolysis in hexane (with a few drops of NH_4OH) have a 25 to 37% weight loss which corresponds to the formula $Al_2O_3 \cdot 3\,(\pm 1)\,H_2O$. Water molecules are lost below 100° C and OH groups are broken below 300° C (Fig. 3);

(ii) the monoliths synthesized in propanol lose about 40% in weight which corresponds approximately to the formula $Al_2O_3 \cdot 4\,(\pm 0.5)\,H_2O$;

(iii) on the other hand, monoliths prepared in acetone and powder from pH 2 water hydrolysis show higher weight losses, about 60 and 75% respectively, which correspond to the formula $Al_2O_3 \cdot 9$ to $18H_2O$. A weight loss corresponding to loss of OH is observed between 200 and 500° C.

If we examine the DSC traces, only pH 9 gel exhibits

a marked high-temperature peak ($\simeq 240°$ C) corresponding to loss of OH. This indicates that large quantities of the "water" of the formula consist both in "zeolithic" water soaked in the pores of the inorganic polymer network and of OH branches. However, it is well established that gels are highly porous [3, 4, 8] and that soaking the pores with solvent favours optical clarity. Chane-Ching and Klein [21] and Yoldas [22] have measured the porosity of some alumina and mullite gels. The size of the pores is typically between 3 and 8 nm and the porosity reaches 65%. The various values of DSC enthalpies indicate various types of "water" and this point will be discussed further with the infrared analysis.

Fig. 4 compares X-ray powder patterns of gels (the monoliths were ground). As expected from DSC and TGA traces, the pH 9 powder is made of crystalline bayerite ($Al(OH)_3$ or $Al_2O_3 \cdot 3H_2O$ [23]. The other broad peaks of the pattern can be assigned to a boehmite-like structure (AlOOH or $Al_2O_3 \cdot 1H_2O$). However, the peaks are very broad and the first one has a larger d-value (0.70 to 0.72 nm) than is usually observed. A similar broad X-ray pattern is observed for pH 2 powder and for some monoliths. Monoliths synthesized using acetone or propanol are different but show amorphous-like patterns (diaspore traces are consistent with the pattern of gels prepared in hexane, propanol and with the Godwa method). Even in the case of boehmite-like material the low intensity of the spectra indicates poor crystallized structures. The large bumps of the acetone route are typical of amorphous samples. However, the broad peak pattern corresponds to the main peaks of gibbsite and of γ-Al_2O_3 structures. In all the cases, our X-ray patterns are broader than is usually observed for such hydrates which can arise either from the particle size (nanomaterials) or the local disorder, or for both reasons. Note that the low-angle diffuse scattering depends largely on the method.

Comparison of the different TGA traces confirms this point of view: the pH 9 powder and to some extent the pH 2 powder show a weight loss jump whereas other materials have a nearly regular loss up to 300° C ($\Delta P \sim 30\%$) and a residual loss between 300 and 500° C ($\Delta P \leqslant 8\%$).

3.2. Structure of alumina "gels"

Figs 5 and 6 show the Raman and infrared (IR) spectra of gel monoliths and powders. The main frequencies are given in Table II. According to X-ray diffraction, the pH 9 powder is mainly constituted of $Al(OH)_3$ (characteristic bands at 380 and 575 cm^{-1} in Raman, 1035 cm^{-1} in IR [24–26]) with boehmite traces (characteristic bands at 360 cm^{-1} in Raman, 365, 480, 630 and 1080 cm^{-1} in IR [26–28]). But some IR bands (520, 570 and 970 cm^{-1}) indicate possible α-AlOOH diaspore traces [25, 28]. They correspond to the 340 and 1060 to 1100 cm^{-1} Raman bands. The IR spectra of pH 2 powder are characteristic of γ-AlOOH boehmite with perhaps some α-AlOOH traces (band at 960 cm^{-1} and shoulders at 670 and 520 cm^{-1}). The intense 360 cm^{-1} Raman band and the weak band at 500 cm^{-1} are also consistent with the presence of

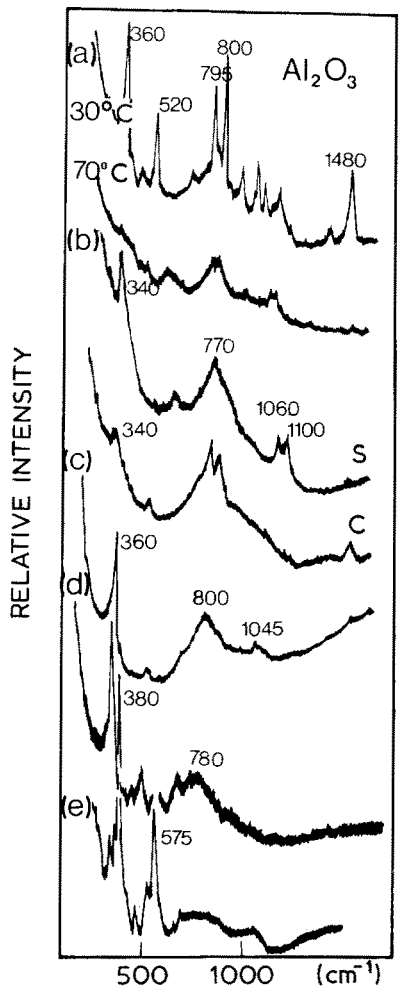

Figure 5 Room-temperature Raman spectra of optically clear monolithic gels (a, b, c) and gel powders (d, e) prepared by various methods: (a) monoliths prepared directly from very slow Al–O–Bu hydrolysis, dried at 30 and 70° C, respectively; (b) monoliths prepared from slow hydrolysis of Al–O–Bu in hexane, surface (S) and core (C), respectively; (c) Godwa monolith; powder prepared by rapid hydrolysis of Al–O–Bu diluted in propanol with pH 2 (d) or pH 9 (e) water.

boehmite. Except in the case of acetone synthesis, IR and Raman spectra of monoliths thus show the characteristic bands of diaspore and boehmite traces.

Raman examination of the core of the monolith (Fig. 5), which can remain incompletely hydrolysed shows well-defined bands between 600 and 1200 cm^{-1} and an intense band at 360 cm^{-1}. The 1480 and 2950 cm^{-1} bands correspond to torsion and stretching modes of CH_3 branches of the incompletely hydrolysed butoxide or of the solvent. The 795, 840 cm^{-1} doublet and the 935 and 1015 cm^{-1} bands can also be assigned to butoxide (partly or unhydrolysed) whereas the 520 cm^{-1} band arises from butanol traces. The broad feature between 500 and 1000 cm^{-1} cannot be related to known alumina hydrates.

Such broad spectra are observed on thermally treated samples of various compositions (Figs 7 and 8): (i) pure alumina gels heated below 1100° C; (ii) mullite gels heated below 1100° C; (iii) cubic phase resulting from the heating of kaolin above 1000° C; (iii) amorphous spinel film prepared by radio-frequency sputtering of Al_2O_3 and Mg^{2+} ion implantation [29], and (iv) transition aluminas [30–34]. All these compounds have a spinel-like structure with

TABLE II IR and Raman frequencies of $Al_2O_3 \cdot nH_2O$ materials in the 200 to 1500 cm^{-1} range

Assignments	Compounds												
	"pH 9"		"pH 2"		"Direct"			"Hexane"		"Acetone"		"Godwa"	
	R	IR	R	IR	R*	R	IR	R	IR	R	IR	R	IR
											1220 w		
	1100 w, b				1125 w						1140 m, b		
		1075 m		1080 m		1080 m	1080 m	1100 w					
		1035 m			1055 w	1050 m	1030 w	1060 w	1030 w		1030 w	1045 w, b	1070 m
					1015 w						990 m		
νAl–OH		970 m		970 m		960 w	970 m		970 m		970 w		960 w
				940 m	935 w						950 w		935 w
		925 w		925 w					915 w				915 w
		890 w		890 w			890 w		890 w	900 m, b	910 m		895 w
	825 w, b	845 w		845 m	840 m			810 s, h	845 w	825 s, b	815 w		
(νAl–O–Bu)					795 m							800 s, b	
νAl–O–Al			780 w, b	770 w	780 m, b	800 m, b		770 s, b					
	705 w		690 w, b		695 w								
				630 m							620 w		625 s, b
		600 m	605 w										
	575 m	560 sh		570 m				585 w					570 m
	525 w	530 m	505 w	500 m	520 m	550 w, b	560 m, b		560 m, b		540 m, b		
								495 w				500 w	
	465 w	470		470 sh	460 w	460 w							480 s, b
		430 w											
		410 w											
	380 s			395 sh								380 sh	
		360 m	360 s	365 s	360 s	360 w, b				360 s, b		360 s	365 m
	350 w	340 w						340 w					
δAl–O	325 w	320 sh		315 sh									325 sh
	260 sh							235 w		275 m, b			

s, strong; m, medium; w, weak; v, very; b, broad; sh, shoulder.
*Incompletely hydrolysed.

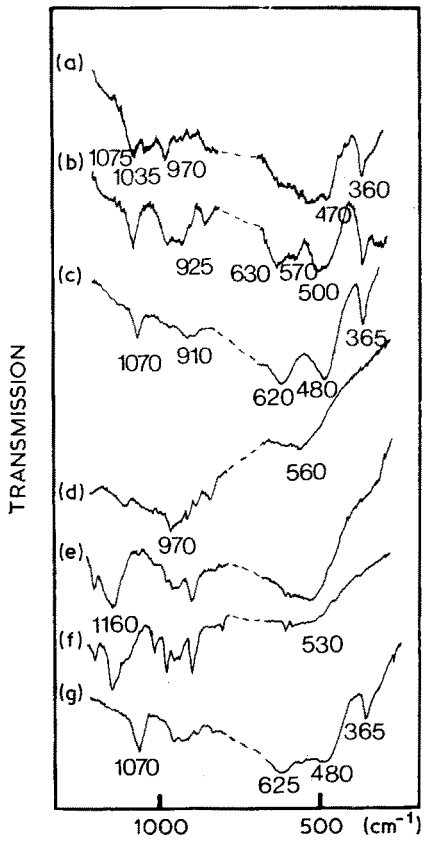

Figure 6 Room-temperature IR spectra of (a) pH 9 and (b) pH 2 powders and of powdered monoliths prepared in hexane ((c) rapidly and (d) slowly) or in acetone ((e) rapidly and (f) slowly). Spectrum of a Godwa sample is given in (g).

AlO_4 tetrahedra and aluminium ions in octahedral sites. Moreover, "ordered" spinel-like structure (for instance β/β'' Al_2O_3 [34–36], $MgAl_2O_4$ [37]) and crystalline mullite [38, 39] show vibrational spectra with (well-) defined bands in the same frequency range.

The apparent density of $Al_2O_3 \cdot nH_2O$ "gels" measured on compacted pellets ranges between 2.2 for

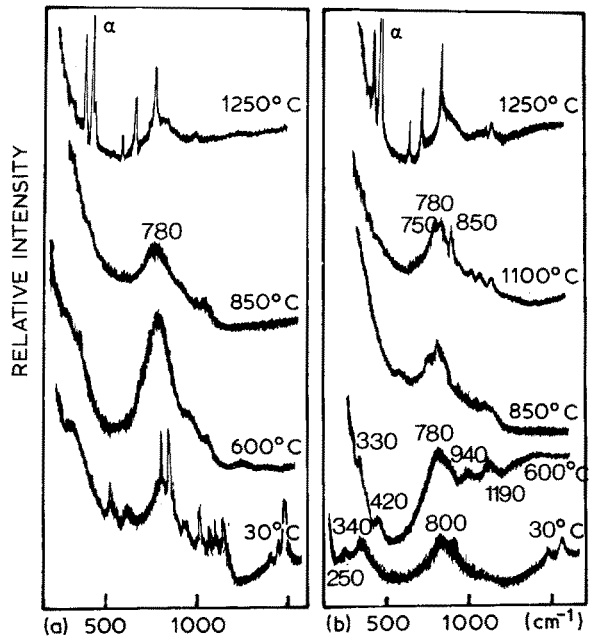

Figure 7 Micro-Raman spectra of monoliths prepared (a) slowly in hexane or (b) rapidly in acetone and heated (2 d) at various temperatures.

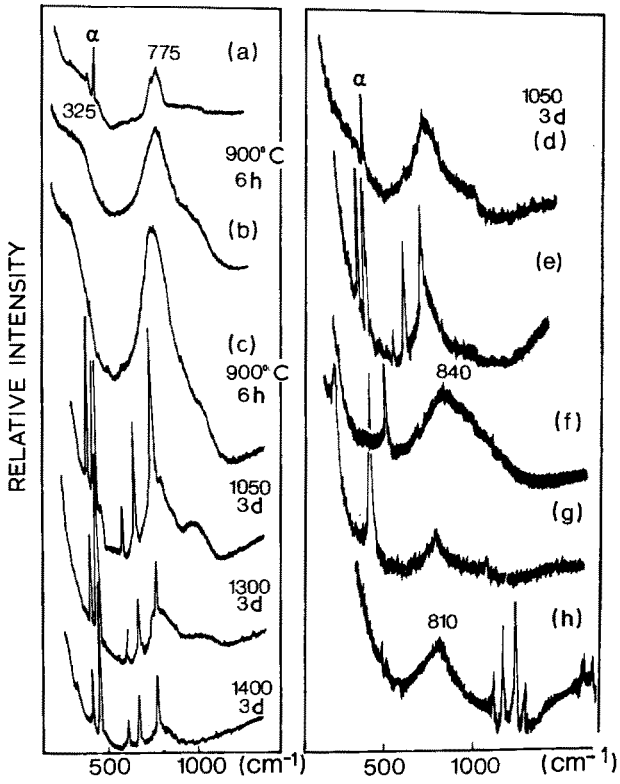

Figure 8 Micro-Raman spectra of amorphous spinel-like structures synthesized by (a) thin film prepared by r.f. sputtering of alumina and Mg^{2+} ion implantation ("sapphire" substrate) [29]; (b) mullite glass prepared by slow hydrolysis of aluminium sec-butoxide and silicon methoxide in hexane [39]; (c) Godwa monolith heated at various temperatures; (d) pH 9 and (e) pH 2 powder heated at 1050° C for 3 d, respectively; (f) metakaolinite from kaolin heated at 1050° C; (g) disordered crystobalite produced from sol–gel synthesis is given for comparison; (h) spinel-like transition alumina single crystal prepared by heating β-alumina single crystal at 850° C [34].

pH 9 powder and 1.3 for monoliths synthesized with acetone as solvent. The density of other monoliths varies between 1.5 and 1.9. This last density represents nearly 80% of the gibbsite density, 60% of the diaspore density and only 50% of the spinel density. These results imply a large porosity, as is well known in such materials [21, 22]. The gel synthesized in acetone must be highly porous, whereas monoliths prepared by very slow hydrolysis of pure Al-butoxide (and in solution in hexane) exhibit the highest density.

3.2.1. Protonic species

Fig. 9 shows IR spectra in the OH stretching and bending regions. According to the crystalline state of $Al(OH)_3$ powder, well-defined bands are observed for pH 9 powder at 3658, 3610, 3590, 3540, 3520, 3405, 3412 and broad bumps at 3300 and 3050 cm^{-1}. The frequencies are rather different from those of well-crystallized bayerite [24], nordstrandite [24], hydrargillite [32, 33] and of gibbsite [26]. This clearly indicates modification of the local structure. The presence of the broad bumps and of the water molecule bending mode at about 1640 cm^{-1} indicates that another hydrate form is present, according to the X-ray analysis. The other compounds show only the broad bumps. These bands can be assigned to the stretching mode of OH in boehmite [29] but their broadness is larger than usually observed, which indicates a great local disorder according to X-ray analysis. The

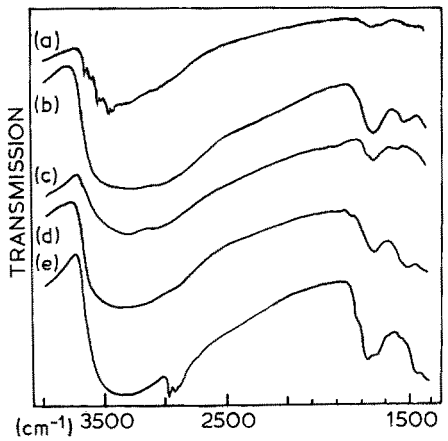

Figure 9 Room-temperature IR spectra in the OH bending and stretching regions of (a) pH 9 and (b) pH 2 powders and of powdered monoliths prepared (d) in cyclohexane or (e) in acetone. Spectrum of a pH 2 powder heated at 200° C is given in (c).

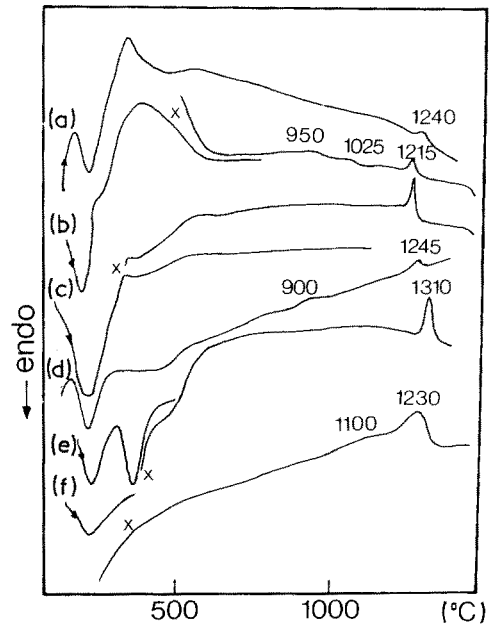

Figure 10 DTA traces of monoliths and powders: (a) monolith synthesized directly from Al-butoxide, (b) monolith synthesized in acetone, (c) in hexane with a few drops of CH_3COOH, (d) pH 2 powder, (e) pH 9 powder and (f) Godwa monolith. Low sensitivity traces are given in the low-temperature region (heating rate 20° C min^{-1}).

presence of water molecules is clearly shown with the 1630 to 1650 cm^{-1} bands. Yellow gels made in acetone show also organic traces (νCH_3 at 2880, 2920 and 2960 cm^{-1}, $\nu C=O$ at 1705 cm^{-1}).

The γ-OH modes are observed in the 1000 to 1300 cm^{-1} region, both on IR and Raman spectra as usually observed for hydrates [24–30, 40] and for transition alumina "single crystals" prepared by heating of protonic β/β'' aluminas. The syntaxic transformation of β/β'' alumina in spinel occurs with the formation of stacking faults. In the planes the order is retained [34, 41–44] and a spinel form containing large quantities of protons is formed. In IR, the 1070 cm^{-1} band is observed for all the materials, except for the gel synthesized in acetone. In this last case a broad 1160 cm^{-1} band is visible. It may correspond to a γ-OH mode under other hydrogen bonding conditions, but the absence of a visible Raman band in the same region does not allow us to give a more precise assignment.

As a preliminary conclusion, alumina "gels" are constituted of a "quasi-amorphous", open Al_2O_3 oxide network having a similar local structure to γ-Al_2O_3, but with alumina hydroxide traces (α- or γ-AlOOH), probably at the surface or in the pores. Rapid hydrolysis leads to crystalline $Al(OH)_3$ traces. Different kinds of hydrogen-bonded water are present in the pores. Acetone as solvent is particularly efficient in reducing the hydrolysis time without formation of crystalline precipitates. This can be related to the ability of acetone to make hydrogen bonds with water and to form intermediate by trans esterification and chelation. Thus the competition between this reaction and the hydrolysis of butoxide regulates the process, leading to optically clear and amorphous monoliths. The high content of "water" in the final gel indicates a very open polymeric network.

3.2.2. Spectra assignments of internal Al–O modes

Corundum (α-Al_2O_3) [41], spinel ($MgAl_2O_4$) [37] and β/β'' Al_2O_3 [36] IR and Raman spectra are well known and assignments have been previously discussed. The study of the conversion of protonic β/β'' aluminas into α-alumina via transition aluminas is also useful to propose an assignment of disordered spinel-like structure [34, 42–44].

The $Al(OH)_3$ structure can be described as an AlO_6 octahedra chain made with OH groups. The AlOOH structure can be described as a slab of corner-shared AlO_6 octahedra, the up and down oxygen of the octahedron having the proton. The intense 380 (360 to 340) cm^{-1} Raman band has been assigned to a motion of the Al–O chain (slab) or in other words to an Al–O bending mode. The stretching Al–O modes of the octahedron are found in the 500 to 600 cm^{-1} range [25, 27, 28]. By comparison with material having the spinel-like structure [30, 32–35] (including the mullite structure [34–38, 45, 48]) the stretching Al–O modes are expected in the 550 to 850 and 750 to 850 cm^{-1} ranges, for the AlO_6 octahedron and AlO_4 tetrahedron, respectively. The corresponding bending modes are expected in the 320 to 450 and 250 to 300 cm^{-1} ranges, respectively (Table II).

3.3. Glass formation and crystallization

Fig. 10 shows DTA traces of typical samples. Exothermic peaks are observed at about 400° C (the combustion of organic traces) in the case of monoliths synthesized directly from aluminium butoxide or in acetone. Small exothermic features are observed between 900 and 1310° C as a function of the preparation conditions. X-ray powder patterns of samples heated between 500 and 1200° C are shown in Fig. 11. The sample differences disappear on heating and γ-alumina pattern is always obtained. However, it is difficult to determine whether or not the θ phase is formed. The high-temperature exothermic peak corresponds to the formation of the α-alumina phase. The better crystallized γ-alumina phase is observed for pH 9 (bayerite) powder. On the contrary, monoliths

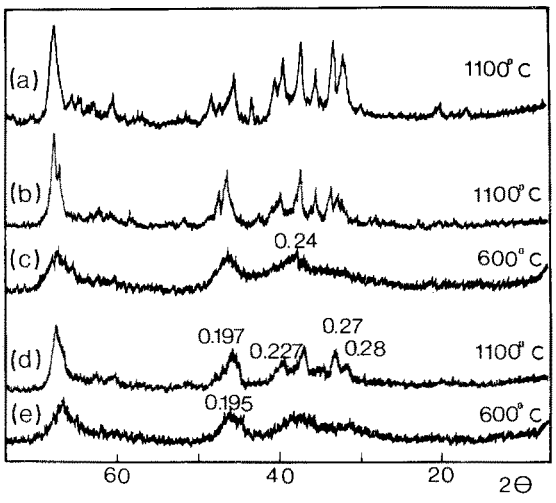

Figure 11 X-ray powder patterns ($\lambda CuK\alpha$) of (a) pH 9 powder and of monoliths synthesized (b, c) in acetone and (d, e) in hexane heated for 1 d at various temperatures.

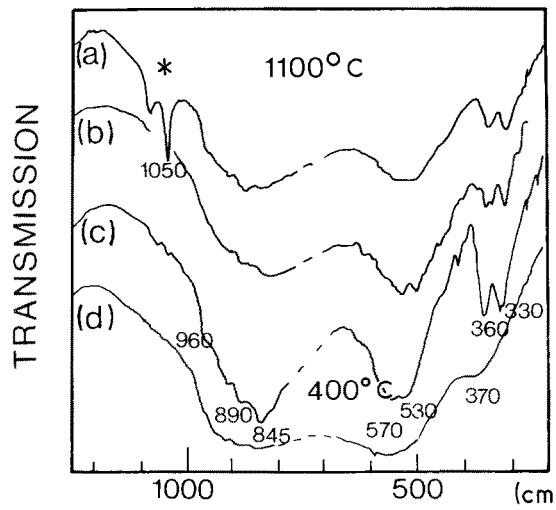

Figure 12 Infrared spectra of spinel-like phase (a, b, c) and "alumina glass" (d) obtained by thermal treatments (2 d) at 1100 and 400° C, respectively; monoliths synthesized slowly in hexane (a, d) and rapidly in acetone (b); pH 9 powder (c). (*) δOH bands which appear after exposure to room-temperature atmospheric moisture.

already having a spinel-like phase in the gel state remain highly disordered but are transformed to α-alumina at lower temperatures. Monoliths remain optically clear up to about 900° C [6]. The loss of clarity is consistent with a nucleation of α-alumina in many places.

Comparison of IR (Fig. 12) and Raman spectra (Figs 7 and 8) allows an understanding of the structural evolution. Below 900° C, the vibrational spectra are not strongly modified, in either the Al–O stretching or bending regions. This indicates that the local structure is less modified. This is consistent with the conservation of the optical clarity. However, the regular narrowing of the X-ray powder pattern and its condensation into γ-alumina-like pattern indicates an increase in long-range correlations. IR and Raman spectra of monoliths synthesized in acetone and heated at about 1100° C show more structured bands (Figs 7 and 12, Table III). The DTA trace shows various anomalies of low intensity (Fig. 10). This may be due to the formation of the intermediate θ-phase.

The formation of the α-alumina phase occurs by growing on the spinel phase as observed for the protonic β/β'' alumina → spinel → α-alumina sequence [39, 43, 47]. The increasing intensity of the α-alumina spectrum as well as a symmetrical decrease of the spinel spectrum are simultaneously observed. According to DTA traces, a large temperature shift is observed for the different methods. Complete conversion into corundum is observed above 1300° C for pH 9 powder (bayerite) whereas conversion of pH 2 (boehmite) powder begins below 1050° C according to previous studies [30]. The intensity of α-alumina traces in γ-alumina samples heated at 1000° C can thus be a measure of the initial boehmite-like traces in the gel.

TABLE III IR and Raman frequencies of alumina, glass and spinel-like phase

Assignment	Compounds			
	"Glass"*		"Spinel"†	
	R	IR	R	IR
			(1100 w)‡	(1085 w)‡
	1060 w		(1035 w)‡	(1050 w)‡
νAl–O–H	1000 sh		990 w	
	950 w, b	925 sh		935 w
		915 v, w		915 w
		890 v, w	860 m	890 m
		850 s, b	825 sh	840 m
νAl–O	800 m, b	845 v, w	800 m, b	
			770 m, b	
				625 w
				610 w
		560 s, b		585 sh
				540 m
				510 m
	460 w	470 m, b	460 w, b	460 w
				415 w
				410 w
δAl–O	350 w, b			370 w
				365 m
				350 m
				322 m
				295 v, w

*Heated at 400° C.
†Heated at 1100° C.
‡Bands observed after exposure to atmospheric moisture.
s, strong; m, medium; w, weak; v, very; sh, shoulder, b, broad.

4. Conclusions

Various kinds of $Al_2O_3 \cdot nH_2O$ materials can be obtained from aluminium sec-butoxide hydrolysis. Rapid hydrolysis lead to crystalline gibbsite ($Al(OH)_3$) or boehmite-like materials (AlOOH) for high and low pH, respectively. On the other hand, by regular and slow hydrolysis, optically clear, amorphous monoliths having a spinel-like local structure are obtained. The use of a solvent such as acetone allows reduction of the hydrolysis time from 6 mon to 1 d. The general formula of the monoliths is $Al_2O_3 \cdot 4$ to $18H_2O$ and AlOOH traces are possible at the polymer surface whereas uncompletely hydrolysed butoxide can be soaked into the core of monoliths. Apparent density lies between 1.3 and 1.9 which corresponds to a high porosity (> 60%). Monoliths remain optically clear up to 900° C and the true γ-alumina phase is gradually formed between 600 and 1100° C as the pores close. Optically clear samples heated between 300 and

600° C can thus be called "alumina glass". Corundum phase nucleates between 1000 and 1300° C as a function of the synthesis method: α-alumina is formed above 1050, 1300 and between 1100 and 1200° C, for boehmite, gibbsite and "alumina glasses", respectively.

Acknowledgement

Mrs N. Blanchard is thanked for her technical assistance.

Note added in proof

The author has cited further details of [9] in:

Idem, Ceramics Int. **15** (1989) 23.

References

1. S. SAKKA and K. KAMIYA, *J. Non-Crystalline Solids* **42** (1980) 403.
2. D. W. JOHNSON Jr, *Amer. Ceram. Soc. Bull.* **64** (1985) 1587.
3. L. L. HENCH and D. R. ULRICH (ed.), "Ultrastructure Processing of Ceramics, Glasses and Composites" (Wiley, New York, 1984).
4. J. ZARZYCKI (ed.), "Proceedings of the International Workshop on Glasses and Glass-Ceramic from Gels", Montpellier, 12–14 September (1985), *J. Non-Crystalline Solids* **82** (1986).
5. K. S. MAZDIYASNI, *Ceram. Int.* **8** (1982) 42.
6. O. BOUQUIN, N. BLANCHARD and Ph. COLOMBAN, "Low Temperature Sintering through Sol-Gel Routes", High Tech Ceramics, edited by P. Vincenzini (Elsevier Science, Amsterdam, 1987) pp. 717–26.
7. L. C. KLEIN, *Ann. Rev. Mater. Sci.* **15** (1985) 227.
8. *Idem*, "Sol-Gel Technology" (Noyes, New Jersey, 1988).
9. Ph. COLOMBAN, *Adv. Ceram.* **21** (1987) 139.
10. *Idem, Solid State Ionics* **21** (1986) 97.
11. B. E. YOLDAS and D. P. PARLOW, *Amer. Ceram. Soc. Bull.* **59** (1980) 640.
12. A. C. PIERRE and D. R. UHLMANN, *J. Amer. Ceram. Soc.* **70** (1987) 28.
13. J-Y. CHANE-CHING and L. C. KLEIN, *ibid.* **71** (1988) 83.
14. A. BERTOLLUZA, C. FAGNANO, M. A. MORELLI, V. GOTTARDI and M. GUGLIEMI, *J. Non-Crystalline Solids* **82** (1986) 127.
15. D. M. KROL, C. A. M. MULDER and J. G. VAN LIEROP, *ibid.* **86** (1986) 241.
16. L. C. KLEIN and G. KORDAS, "Electron Spin Resonance and Other Spectroscopies Used in Characterizing Sol-Gel Processing", Materials Research Society Symposium Proceedings, Vol. 73 (Materials Research Society, Pittsburgh, 1986) p. 461.
17. I. ARTAKI, T. W. ZERDA and J. JONAS, *J. Non-Crystalline Solids* **81** (1986) 381.
18. G. E. WALRAFEN, M. S. HOKMABADI, N. C. HOLMES, W. J. NELLIS and S. HENNINGS, *J. Chem. Phys.* **82** (1985) 2472.
19. R. K. DWIVEDI and G. GODWA, *J. Mater. Sci. Lett.* **4** (1985) 331.
20. B. E. YOLDAS, *Amer. Ceram. Soc. Bull.* **54** (1975) 289.
21. J. Y. CHANE-CHING and L. C. KLEIN, *J. Amer. Ceram. Soc.* **71** (1988) 86.
22. B. E. YOLDAS, *Amer. Ceram. Soc. Bull.* **59** (1980) 479.
23. Powder Diffraction File, Data Book JCPDS (International Centre for Diffraction Data, Swarthmore, 1986).
24. D. VIVIEN, M. C. STAGMANN and C. MAZIERES, *J. Chimie Physique* **10** (1973) 1502.
25. S. CRESTIN-DESJOBERT, F. ORUEGE and R. GOUT, *Terra Cognita* **7** (1987) 14.
26. C. KARR Jr, "IR and Raman Spectroscopies of Lunar and Terrestrial Materials" (Academic, New York, 1975) Chs 8 and 9.
27. A. B. KISS, G. KERESZTURY and L. FARKAS, *Spectrochim. Acta* **36A** (1980) 653.
28. P. FORBES, J. DUBESSY and C. KOSZTOLANYI, *Terra Cognita* **7** (1987) 16.
29. Ph. SCHNELL, G. VELASCO and Ph. COLOMBAN, *Solid State Ionics* **5** (1981) 242.
30. M. C. STAGMANN, D. VIVIEN and C. MAZIÈRES, *Spectrochim. Acta* **29A** (1973) 1653.
31. M. C. STEGMANN, D. VIVIEN and C. MAZIÈRES, *J. Chimie Physique* **71** (1974) 761.
32. P. P. MARDILOVICH, A. I. TROKHIMETS and M. V. ZORETSHIC, *Z. Prikladnui Spektroskopii* **40** (1984) 401.
33. P. P. MARDILOVICH and A. I. TROKHIMETS, *ibid.* **36** (1982) 258.
34. Ph. COLOMBAN, *J. Mater. Sci. Lett.* **7** (1988) 1324.
35. Ph. COLOMBAN and G. LUCAZEAU, *J. Chem. Phys.* **72** (1980) 1213.
36. D. DOHY, G. LUCAZEAU and D. BOUGEARD, *Solid State Ionics* **11** (1983) 1.
37. P. McMILLAN and M. AKAOGI, *Amer. Mineral.* **72** (1987) 361.
38. P. McMILLAN and B. PIRIOU, *J. Non-Crystalline Solids* **53** (1982) 279.
39. Ph. COLOMBAN, *J. Mater. Sci.* **24** (1989).
40. Ph. COLOMBAN and A. NOVAK, *J. Molec. Struct.* **177** (1988) 277.
41. S. P. PORTO and R. S. KRISHNAM, *J. Chem. Phys.* **47** (1967) 1009.
42. N. BAFFIER, J. C. BADOT and Ph. COLOMBAN, *Solid State Ionics* **11** (1983) 157.
43. Ph. COLOMBAN, J. P. BOILOT, A. KAHN and G. LUCAZEAU, *Nouveau J. Chimie* **2** (1978) 21.
44. P. LENFANT, D. PLAS, M. RUFFO and Ph. COLOMBAN, *Mater. Res. Bull.* **15** (1980) 1817.
45. K. IISHII, E. SALJE and Ch. WERNEKE, *Phys. Chem. Minerals* **4** (1979) 173.
46. E. SALJE and Chr. WERNEKE, *Contr. Minerals Petrol.* **79** (1982) 56.
47. H. SAALFELD, H. MATHIES and S. K. DATTA, *Ber. Dtsch. Keram. Ges.* **45** (1968) 212.
48. Ph. COLOMBAN, "Gel-glass-mullite Transition as a Function of Powder Preparation, Stoichiometry and Zr(Ti) Addition", Proceedings of the 2nd International Conference on Ceramic Powder Processing Science, 12–14 October (1988) Berchtesgoden.

Received 28 April
and accepted 8 September 1988